PALEOCEANOGRAPHY, VOL. 28, 517–528, doi:10.1002/palo.20048, 2013

In situ $\delta^{18}O$ and Mg/Ca analyses of diagenetic and planktic foraminiferal calcite preserved in a deep-sea record of the Paleocene-Eocene thermal maximum

Reinhard Kozdon,[1] D. C. Kelly,[1] K. Kitajima,[1] A. Strickland,[1] J. H. Fournelle,[1] and J. W. Valley[1]

Received 21 May 2013; revised 12 August 2013; accepted 22 August 2013; published 17 September 2013.

[1] We report $\delta^{18}O$ and minor element (Mg/Ca, Sr/Ca) data acquired by high-resolution, in situ secondary ion mass spectrometry (SIMS) from planktic foraminiferal shells and 100–500 μm sized diagenetic crystallites recovered from a deep-sea record (ODP Site 865) of the Paleocene-Eocene thermal maximum (PETM). The $\delta^{18}O$ of crystallites (~1.2‰ Pee Dee Belemnite (PDB)) is ~4.8‰ higher than that of planktic foraminiferal calcite (−3.6‰ PDB), while crystallite Mg/Ca and Sr/Ca ratios are slightly higher and substantially lower than in planktic foraminiferal calcite, respectively. The focused stratigraphic distribution of the crystallites signals an association with PETM conditions; hence, we attribute their formation to early diagenesis initially sourced by seafloor dissolution (burndown) ensued by reprecipitation at higher carbonate saturation. The Mg/Ca ratios of the crystallites are an order of magnitude lower than those predicted by inorganic precipitation experiments, which may reflect a degree of inheritance from "donor" phases of biogenic calcite that underwent solution in the sediment column. In addition, SIMS $\delta^{18}O$ and electron microprobe Mg/Ca analyses that were taken within a planktic foraminiferal shell yield parallel increases along traverses that coincide with muricae blades on the chamber wall. The parallel $\delta^{18}O$ and Mg/Ca increases indicate a diagenetic origin for the blades, but their $\delta^{18}O$ value (−0.5‰ PDB) is lower than that of crystallites suggesting that these two phases of diagenetic carbonate formed at different times. Finally, we posit that elevated levels of early diagenesis acted in concert with sediment mixing and carbonate dissolution to attenuate the $\delta^{18}O$ decrease signaling PETM warming in "whole-shell" records published for Site 865.

Citation: Kozdon, R., D. C. Kelly, K. Kitajima, A. Strickland, J. H. Fournelle, and J. W. Valley (2013), In situ $\delta^{18}O$ and Mg/Ca analyses of diagenetic and planktic foraminiferal calcite preserved in a deep-sea record of the Paleocene-Eocene thermal maximum, *Paleoceanography*, *28*, 517–528, doi:10.1002/palo.20048.

1. Introduction

[2] Oxygen isotope ($\delta^{18}O$) and Mg/Ca ratios of foraminiferal calcite are two of the most widely used geochemical proxies for paleoceanographic reconstructions, yet the fidelity of these records is frequently questioned on the grounds that foraminiferal shells found in deep-sea sediments are susceptible to postdepositional diagenesis [e.g., *Killingley*, 1983]. Cryptic diagenesis is particularly troublesome for planktic foraminiferal $\delta^{18}O$ records from tropical locations where the surface-to-bottom temperature gradients are most pronounced [*Pearson*, 2012]. For instance, planktic foraminiferal shells originally grown at warm (>20°C) sea surface temperatures (SSTs) may be partly recrystallized and/or have diagenetic calcite added to them at much colder (<5°C) bottom water temperatures once deposited on the seafloor. Under such settings, the $\delta^{18}O$ of diagenetic calcite may be up to ~6‰ higher than that of biogenic calcite; hence, even minor postdepositional alteration can shift the $\delta^{18}O$ of shells toward higher values and underestimate SSTs [e.g., *Matthews and Poore*, 1980]. This view is supported by the detailed examination of planktic foraminiferal shells recovered from Paleogene deep-sea sediments, which has shown that postdepositional diagenesis imparts a "frosty" hue [*Sexton et al*., 2006] to the specimens and elevates whole-shell $\delta^{18}O$ values [e.g., *Pearson et al*., 2007; *Pearson and Burgess*, 2008].

[3] One approach to minimizing the effects of diagenesis on tropical SST records is to use geochemical data derived from exceptionally well-preserved, "glassy" planktic foraminiferal shells recovered from clay-rich marine sediments. Over the years, $\delta^{18}O$ data acquired from glassy shells have revealed that tropical SSTs during the Cretaceous and Paleogene greenhouse climate states were warmer than originally perceived [e.g., *Norris and Wilson*, 1998; *Pearson*

Additional supporting information may be found in the online version of this article.

[1]WiscSIMS, Department of Geoscience, University of Wisconsin-Madison, Madison, Wisconsin, USA.

Corresponding author: R. Kozdon, WiscSIMS, Department of Geoscience, University of Wisconsin-Madison, 1215 W. Dayton St., Madison, WI 53706, USA. (rkozdon@geology.wisc.edu)

©2013. American Geophysical Union. All Rights Reserved.
0883-8305/13/10.1002/palo.20048

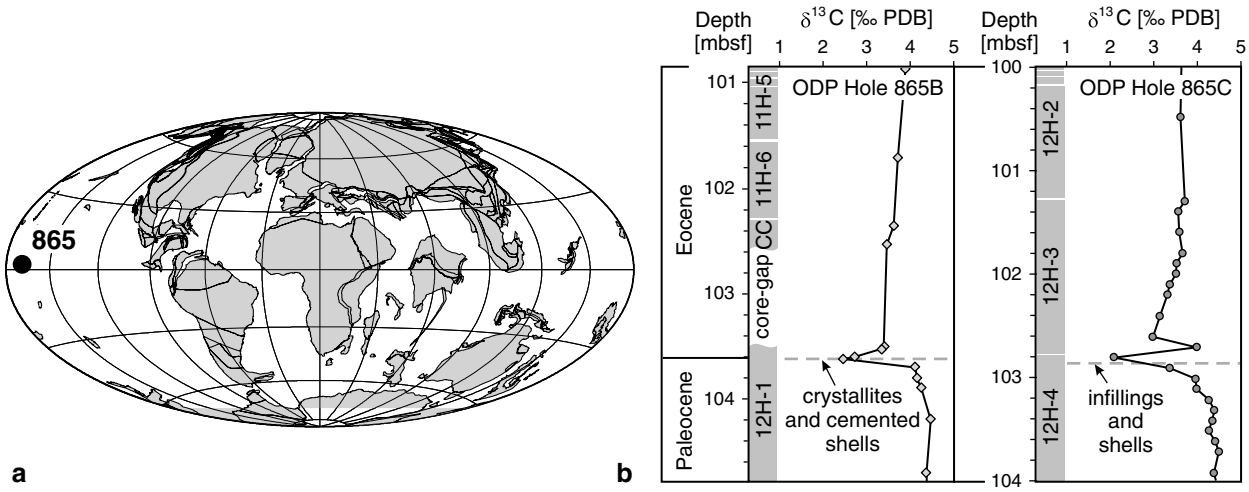

Figure 1. (a) Map showing early Eocene paleogeography (http://www.odsn.de/odsn/services/paleomap/paleomap.html) and location of Site 865. (b) Correlation of the PETM sections recovered from holes 865B and 865C using the CIE recorded by planktic foraminiferal shells [*Bralower et al*., 1995]. The diagenetic crystallites and planktic foraminiferal shells used in this study are from near the base of the CIE (crystallites and cemented shells: hole 865B, 103.60 mbsf; diagenetic infillings and foraminiferal shells: hole 865C, 102.86 and 102.90 mbsf). Note truncation of uppermost part of hole 865B PETM record by coring gap.

et al., 2001; *Wilson and Norris*, 2001; *Wilson et al*., 2002; *Zachos et al*., 2006]. As a consequence, glassy planktic foraminifera have come to be prized as a type of "gold standard" for reconstructing tropical SSTs during past greenhouse climate states. Unfortunately, sample locations preserving glassy planktic foraminifera in the sedimentary record are sporadic and largely limited to nearshore environments that may have been influenced by low $\delta^{18}O$ waters from continental sources.

[4] The limited spatiotemporal occurrence of glassy planktic foraminifera is not well suited for characterizing long-term climate variability on a global scale or monitoring secular changes in the thermal stratification of open ocean environments. On the other hand, pervasive seafloor diagenesis negates the expansive geographic coverage provided by the myriad deep-sea records procured through decades of ocean drilling. This dilemma places a premium on quantifying the effects of diagenesis on foraminiferal shell chemistries; however, direct measurement of the $\delta^{18}O$ and elemental compositions of diagenetic calcite has proven difficult as it typically forms on micrometer scales with only portions of foraminiferal shells being recrystallized (neomorphism) or having diagenetic calcite added (cementation). Previous studies have attempted to correct whole-shell measurements for the effects of diagenesis by mass balance [e.g., *Schrag et al*., 1995; *Schrag*, 1999; *Tripati et al*., 2003], estimating the proportion of diagenetic calcite with a chemical composition similar to that reported from inorganic precipitation experiments [e.g., *Oomori et al*., 1987]. Still it remains unclear if this approach accurately predicts chemical change caused by diagenesis in the sediment column.

[5] An alternative vehicle for accessing the wealth of paleoceanographic information encoded within planktic foraminiferal shells preserved in relatively continuous deep-sea records is the use of high-resolution, in situ techniques such as secondary ion mass spectrometry (SIMS) and electron probe microanalysis (EPMA) to measure the $\delta^{18}O$ and elemental compositions of minute domains within individual shells. In an earlier study [*Kozdon et al*., 2011], $\delta^{18}O$ measurements by SIMS using ~10-μm beam spot sizes and Mg/Ca analysis by EPMA were performed on non-porous, alteration-resistant domains within individual frosty planktic foraminiferal shells recovered from a tropical deep-sea section (Ocean Drilling Program Site 865) straddling the Paleocene-Eocene boundary. It was found that the in situ $\delta^{18}O$ values were comparable to those reported from age-equivalent glassy shells, and up to ~2‰ lower than the "whole-shell" $\delta^{18}O$ values reported for frosty foraminiferal shells from the same core samples. In contrast, the complementary in situ Mg/Ca ratios were indistinguishable from published "whole-shell" Mg/Ca ratios.

[6] Here we reevaluate the effects of postdepositional diagenesis on planktic foraminiferal shell chemistry in the Site 865 section with particular emphasis on its record of a transient global warming event referred to as the Paleocene-Eocene thermal maximum (PETM). Recent advances to SIMS instrumentation and refinements to analytical methods, in combination with improved sample preparation [*Kita et al*., 2009], have made it possible to measure the $\delta^{18}O$ in carbonates in situ with 3 μm beam-spot sizes at the ±0.8‰ level or better [*Kozdon et al*., 2009; *Valley and Kita*, 2009; *Vetter et al*., 2013]. The enhanced spatial resolution afforded by the smaller beam spot permits delineation of $\delta^{18}O$ compositional trends within individual foraminiferal shells recovered from the Site 865 PETM section, allowing identification and analysis of both the biogenic and the diagenetic calcite. Furthermore, the relatively nondestructive nature of SIMS $\delta^{18}O$ measurements permits the acquisition of "paired" in situ elemental abundance data from the same domains within a given foraminiferal shell; hence, parallel EPMA or SIMS measurements are used to acquire complementary Mg/Ca and Sr/Ca ratios. We use these newly acquired data to address fundamental questions regarding the effects of carbonate diagenesis on deep-sea PETM records by comparing

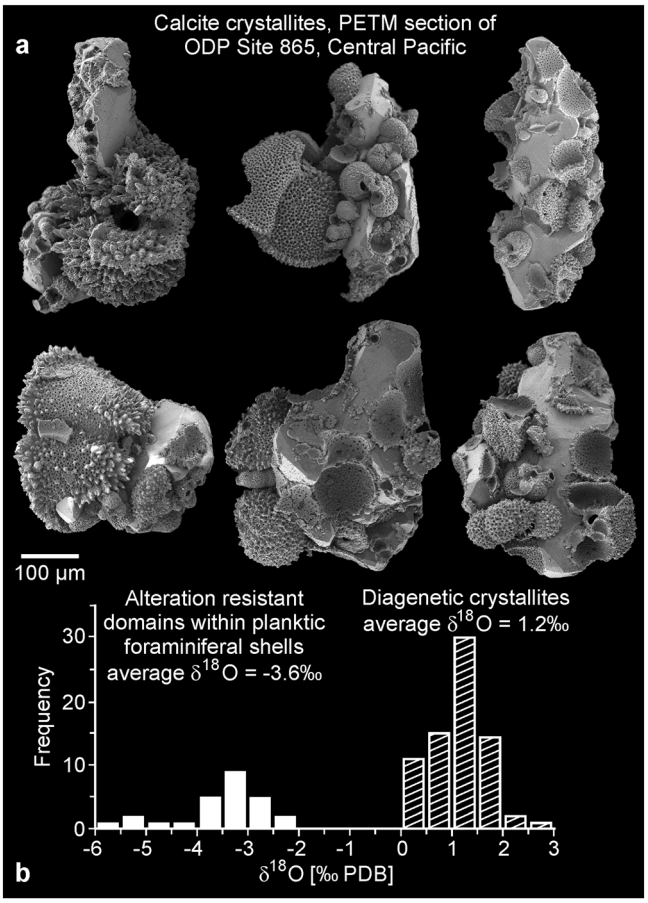

Figure 2. (a) SEM images showing six of the diagenetic crystallites with cemented planktic foraminiferal shells analyzed from PETM sample: hole 865B, 103.60 mbsf. (b) Histograms comparing the $\delta^{18}O$ values measured in situ in polished cross sections of diagenetic crystals (average $\delta^{18}O = 1.2‰$ PDB, $n = 73$) to those measured from relatively unaltered domains in uncemented planktic foraminiferal shells and shell fragments cemented to the crystallites (average $\delta^{18}O = -3.6‰$ PDB, $n = 26$). Note bimodal distribution with a $\Delta^{18}O_{(cement\text{-}shell)}$ of ~4.8‰.

the in situ $\delta^{18}O$ and elemental abundance data (Mg/Ca, Sr/Ca) compiled from individual foraminiferal shells to paired in situ $\delta^{18}O$ and elemental abundance data (Mg/Ca, Sr/Ca) acquired from exceptionally large (~500 µm) diagenetic crystallites recovered from the Site 865 PETM section.

2. Material and Methods

[7] Study materials were collected from two PETM sections recovered at ODP Site 865 (Figure 1a). Both of the PETM sections are composed of foraminiferal nannofossil ooze deposited as part of a pelagic cap atop Allison Guyot in the Mid-Pacific Mountains [*Sager et al*., 1993]. Benthic foraminiferal faunas indicate that the two PETM sections were deposited at mid-bathyal (~1300 m) water depths [*Bralower et al*., 1995], and paleolatitude projections place Site 865 within a few degrees of the equator during the late Paleocene [*Sager et al*., 1993]. Biochemostratigraphic frameworks constructed by previous studies [*Bralower and Mutterlose*, 1995; *Bralower et al*., 1995a; *Kelly et al*., 1996, 1998] have constrained the PETM to a thin (~15–20 cm) interval in the stratigraphic sections recovered from holes 865B (18°26.415′N, 179°33.349′W, 1516.2 m water depth) and 865C (18°26.425′N, 179°33.339′W, 1517.4 m water depth). Sample selection was constrained by the carbon isotope excursion (CIE) marking the PETM, which is signaled by an abrupt ~2‰ decrease in planktic foraminiferal $\delta^{13}C$ values at Site 865 (Figure 1b). Accordingly, one bulk-sediment sample within the CIE interval in the hole 865B section (103.60 m below seafloor (mbsf)) and two within the CIE interval in the hole 865C section (102.86 and 102.90 mbsf) were targeted for study. The calcareous ooze was rinsed with pH buffered (~8.0) deionized water over a 63 µm sieve and oven-dried at ~30°C overnight. Inspection of the >250 µm size fraction revealed the presence of abundant, uncemented foraminiferal shells as well as relatively large (~500 µm diameter) crystallites composed of translucent calcite cementing numerous foraminiferal shells and fragments (Figure 2a). Subsequent inspection of the >63 µm size fraction of pre-CIE and post-CIE core samples confirmed that the stratigraphic occurrence of these relatively large crystallites is confined to the CIE interval. No such crystallites were found in late Paleocene and early Eocene samples outside the PETM interval.

[8] For SIMS and EPMA measurements, individual diagenetic crystallites and planktic foraminiferal shells were cast with two grains of UWC-3 calcite standard ($\delta^{18}O = 12.49‰$ (Vienna standard mean ocean water; VSMOW) [*Kozdon et al*., 2009]) in a 25 mm diameter epoxy mount, ground to the level of best exposure [*Kozdon et al*., 2011], and polished to a relief of less than 1 µm [*Kita et al*., 2009]. In order to minimize instrumental bias related to sample position [*Kita et al*., 2009], each epoxy mount was prepared such that all analytical pits were within 5 mm of the center of the mount. Sample mounts were gold coated for scanning electron microscope (SEM) imaging and SIMS analyses. The gold coating was subsequently removed and a carbon coat applied for EPMA measurements.

2.1. In Situ $\delta^{18}O$ Measurements

[9] In situ oxygen isotope data were acquired from the diagenetic crystallites in the WiscSIMS Laboratory at UW-Madison using a CAMECA IMS-1280 large radius multicollector SIMS [*Kita et al*., 2009; *Valley and Kita*, 2009] with analytical conditions similar to those reported by *Kozdon et al*. [2011]. For the larger spot analyses, a $^{133}Cs^{+}$ primary ion beam with an intensity of ~1.6 nA was focused to a beam-spot size of ~10 µm. The typical secondary $^{16}O^{-}$ ion intensity was 2.4×10^{9} counts per second (cps), and $^{18}O^{-}$ and $^{16}O^{-}$ ions were simultaneously collected by two Faraday cup detectors. Charging of the sample surface was compensated by Au coating and an electron flood gun. Four to six consecutive measurements of UWC-3 calcite standard were performed before and after every set of 5–16 sample analyses. The average precision (reproducibility) for a set of bracketing standard analyses is ±0.22‰ (2 standard deviations, spot-to-spot).

[10] A second analytical setup with a smaller primary beam-spot size of ~3–4 µm and an intensity of 30 pA was used to evaluate $\delta^{18}O$ trends across foraminiferal chamber wall cross sections. The general analytical conditions were

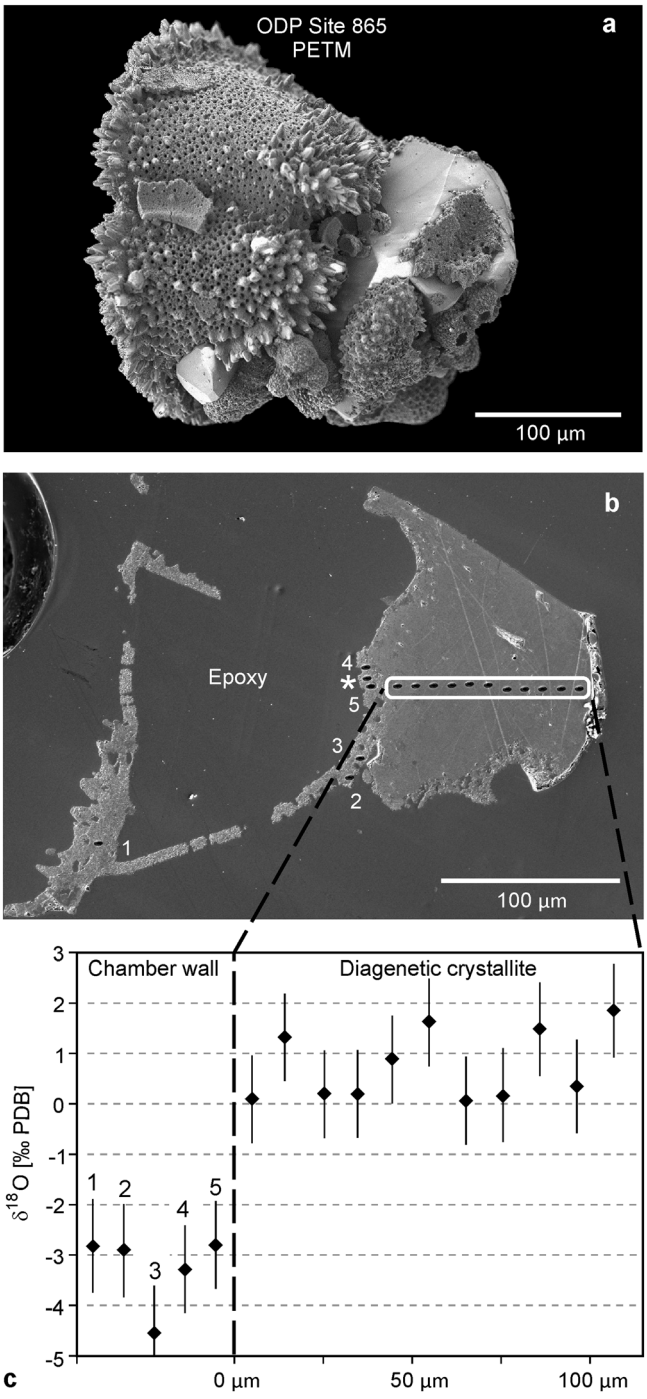

Figure 3. (a) SEM image of a ~100 µm diagenetic crystallite and several smaller calcite overgrowths cemented on a morozovellid shell from PETM sample: hole 865B, 103.60 mbsf. (b) SEM image of the same shell and diagenetic crystallite in polished cross section showing ~3 µm SIMS pits for $\delta^{18}O$ analyses. Measurements in the chamber wall of the foraminiferal shell are numbered 1 to 5, one irregular pit overlapping a pore is marked by an asterisk. (c) Plot of the corresponding $\delta^{18}O$ values. Error bars connote 2 standard deviations. Note the absence of zonation in the 100 µm traverse across the diagenetic crystallite. The $\Delta^{18}O_{(cement\text{-}shell)}$ for this sample is 4‰.

similar to those described by *Kozdon et al*. [2009], and secondary ions were detected simultaneously by a Faraday cup detector ($^{16}O^-$) and a miniaturized Hamamatsu electron multiplier ($^{18}O^-$). Typical secondary $^{16}O^-$ count rates were 2.0×10^7 cps. The gain of the electron multiplier was monitored before the third analysis of each group of four or five standard calcite analyses and, when necessary, the applied high voltage was adjusted to compensate for drift in the gain of the electron multiplier. The average precision (reproducibility) for a set of bracketing standard analyses using the small-spot analytical setup is ±0.8‰ (2 standard deviations, spot-to-spot).

[11] Oxygen isotope ratios of marine carbonates are traditionally expressed relative to Pee Dee Belemnite (PDB). Therefore, final data were converted from calcite $\delta^{18}O$ on the VSMOW scale to the PDB scale using the equation of *Coplen et al*. [1983]:

$$\delta^{18}O[‰PDB] = 0.97002 \times \delta^{18}O[‰VSMOW] - 29.98 \quad (1)$$

After SIMS $\delta^{18}O$ measurements, the appearance of each analysis pit was assessed by SEM imaging. We consider oxygen isotope data from "irregular" pits [*Cavosie et al*., 2005] overlapping epoxy resin, cracks, cavities, and inclusions as possibly compromised, and values from these measurements were excluded from the data set (all data are reported in Table S1 in the supporting information).

2.2. In Situ Mg, Sr, and Ca Measurements

[12] SIMS analyses for minor and major element concentrations (Mg, Sr, and Ca) in the diagenetic crystallites were performed using a primary O^- ion beam with an acceleration voltage of 13 kV (23 kV total acceleration voltage) and an intensity of 1 nA, focused to a ~15 µm beam-spot size. ^{40}Ca was analyzed by a Faraday cup collector and all other elements by an electron multiplier in the monocollection system using five cycles with a counting time of 3 s for ^7Li, ^{11}B, ^{12}C, ^{24}Mg, ^{31}P, ^{32}S, ^{55}Mn, ^{57}Fe, ^{63}Cu, ^{64}Zn, ^{88}Sr, ^{89}Y, and ^{138}Ba and a counting time of 2 s for ^{23}Na and ^{28}Si. Only data for Mg, Sr, and Ca were used in this study. A presputtering time of 60 s was selected, the mass resolving power was set to 7000, and the secondary ion sensitivities were calibrated by measurements of the UWC-3 calcite standard.

[13] In addition, the Mg/Ca ratios of small (<20 µm) domains and traverses crosscutting foraminiferal chamber-wall cross sections were measured using the CAMECA SX51 electron microprobe at the UW-Madison Department of Geoscience. Fully quantitative analyses (mineral standards, background subtracted, and matrix corrected) were performed using Probe for EPMA© software. An accelerating voltage of 15 kV with 10 nA Faraday current and a tightly focused beam were used, with a counting time of 20 s on the peak and 10 s on each of the two background positions. These analyses were performed using the "Time Dependent Intensity" feature of the Probe for EPMA software, where Ca and Mg were measured in 4 s increments and counts were plotted against time, with extrapolation to time = 0 s as the true count rate. The natural carbonate standards Delight Dolomite, Callender Calcite, and UWC-3 were used for Mg and Ca; Mg-Kα X-rays were measured on two spectrometers and aggregated. Carbon was calculated within the matrix correction on an atomic basis as C = (Ca + Mg + Sr).

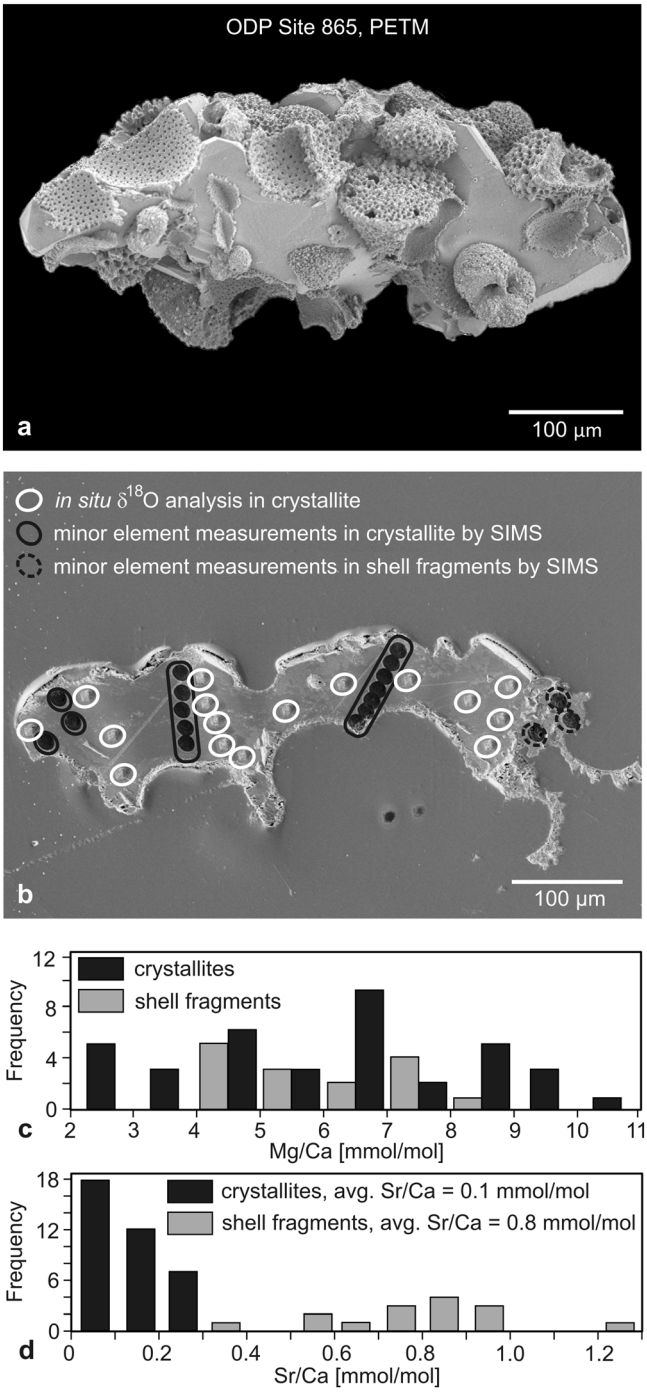

Figure 4. (a) SEM image of a ~500 µm diagenetic crystallite from PETM sample: hole 865B, 103.60 mbsf. (b) Polished cross section of same crystallite showing ~10 µm SIMS analysis pits for $\delta^{18}O$ (white), Mg/Ca and Sr/Ca ratios in the crystallite (black solid line) and cemented foraminiferal shell fragments (black dashed line). (c) Frequency distribution of Mg/Ca ratios measured in five of the diagenetic crystallites (black) and foraminiferal fragments (grey) cemented to these crystallites. (d) Frequency distribution of Sr/Ca ratios measured in five of the diagenetic crystallites (black) and cemented foraminiferal shell fragments (grey).

2.3. Sampling Strategies for In Situ Measurements

[14] A series of discrete SIMS $\delta^{18}O$ measurements were taken along each of several traverses running from the outer edge to the center of six different crystallites as well as along traverses spanning the boundaries between the crystallite edges and cemented planktic foraminiferal shell fragments (Figures 3a, 3b, 4a, and 4b). The shell surfaces of the cemented planktic foraminifera possess mound-like (10–15 µm), pustular outgrowths called "muricae" that are diagnostic of species belonging to the mixed-layer dwelling genera *Morozovella* and *Acarinina* [*Blow*, 1979]. Previous study determined that the basal areas of muricae are optimal targets for 10 µm SIMS beam spots owing to their size in cross section, nonporous textures, and higher resistance to diagenetic alteration [*Kozdon et al*., 2011]. We therefore targeted the basal, mound-like areas of muricae within acarininid and morozovellid fragments cemented to the crystallites (Figures 3b and 5f). An added benefit of in situ SIMS analysis is that most of the original sample material is conserved, permitting the collection of elemental (Mg/Ca, Sr/Ca) ratios via in situ SIMS and/or EPMA measurements along traverses paralleling those constructed for $\delta^{18}O$ analyses (Figure 4b and 5f). Compositional trends in $\delta^{18}O$ and Mg/Ca ratios within an uncemented shell of a planktic foraminifer (*Morozovella velascoensis*) were also delineated along parallel traverses using the smaller SIMS beam-spot size (~3 µm) and EPMA, respectively (Figures 5d–5f).

3. Results

3.1. The $\delta^{18}O$ of Diagenetic Crystallites and Cemented Foraminiferal Shells

[15] The $\delta^{18}O$ of the diagenetic crystallites analyzed using the larger 10 µm SIMS beam-spot averages 1.2‰ (PDB, $n = 73$) with values ranging between 0.1 and 2.9‰ (Figure 2b). None of the crystallites show a systematic zonation along the edge-to-center $\delta^{18}O$ traverses (Figures 3b and 3c). By comparison, the $\delta^{18}O$ measured (3 and 10 µm SIMS beam-spot sizes) in the basal mounds of muricae in the uncemented planktic foraminiferal shell and shell fragments attached to the crystallites averages −3.6‰ ($n = 26$), which is ~4.8‰ lower than the average $\delta^{18}O$ of the digenetic crystallites (Figures 2b and 3c).

3.2. Minor Element Ratios of Large Crystallites and Cemented Shells

[16] The Mg/Ca and Sr/Ca ratios in five of the large crystallites were measured in situ by SIMS along edge-to-center traverses paralleling the SIMS $\delta^{18}O$ analysis pits (Figures 4a and 4b). For comparison, similar measurements were performed on local domains within planktic foraminiferal shell fragments cemented to the crystallites. Unlike the striking $\delta^{18}O$ offset seen between these two substrates ($\Delta^{18}O_{(cement\text{-}shell)} = 4.8‰$), all of the Mg/Ca ratios of the cemented shell fragments (4.4 to 8.7 mmol/mol, $n = 15$) plot within the range of Mg/Ca ratios registered by the crystallites (2.5 to 10.3 mmol/mol, $n = 37$) with both substrates yielding the same average Mg/Ca ratio of 6.2 mmol/mol (Figure 4c). In contrast, Sr/Ca ratios (Figure 4d) in the large crystallites (≤0.3 mmol/mol) are notably lower than in the attached planktic foraminiferal shell fragments (0.3 to 1.2 mmol/mol).

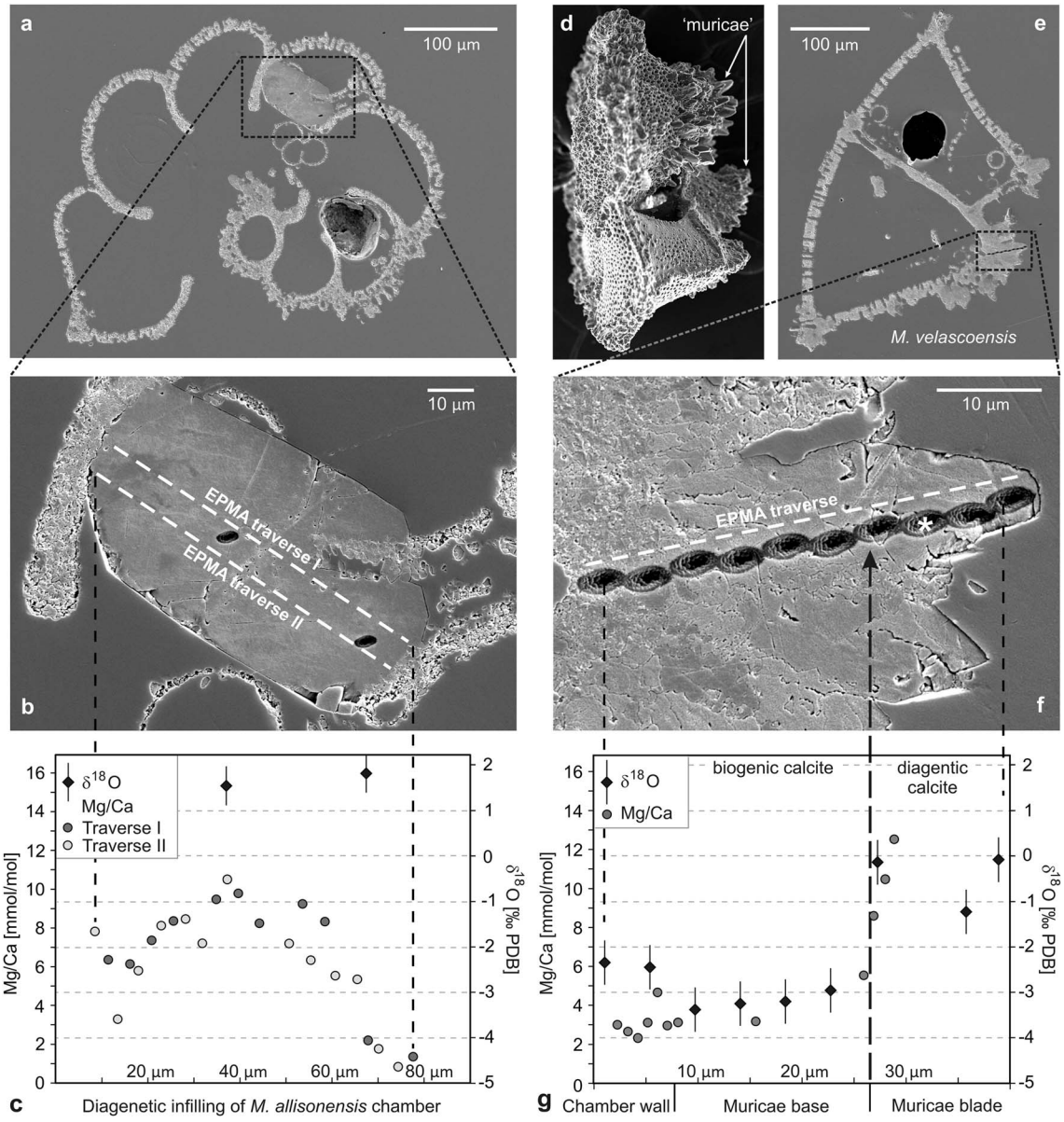

Figure 5. (a) SEM image showing a ~100 µm sized diagenetic crystallite (dashed box) that formed inside a chamber of the PETM morphotype *M. allisonensis* (hole 865C, 102.86 mbsf). (b) Enlargement of the crystallite showing two parallel traverses of EPMA tracks where Mg/Ca analyses were performed. Two SIMS analysis pits for in situ $\delta^{18}O$ are visible in the crystallite. (c) Mg/Ca ratio traverses from Figure 5b delineates a symmetrical decrease from core to rim, and the average $\delta^{18}O$ of 1.4‰ is similar to values measured in the larger crystallites displayed in Figures 2 and 3. Error bars connote 2 standard deviations. (d) SEM image showing 10–15 µm sized calcite blades protruding from pustular muricae coalesced atop the chamber tips of a planktic foraminiferal (*M. velascoensis*) shell from core sample: hole 865C, 102.90 mbsf. (e) SEM image of polished cross section of the same shell shown in Figure 5d. Note traverse of 3 µm SIMS analysis pits delimited by dashed box. (f) Highly magnified SEM image of polished cross section showing parallel traverses of $\delta^{18}O$ SIMS pits (asterisk denotes an irregular pit, see Table S1 in the supporting information) and Mg/Ca ratio EPMA measurements (white dashed line) taken along the major axis of a muricae blade. The volumes sampled for $\delta^{18}O$ by SIMS and Mg/Ca by EPMA are comparable in size. (g) Coherent trends in $\delta^{18}O$ and Mg/Ca delineated by parallel traverses along muricae blade shown in image Figure 5f. The black arrow points to the boundary between biogenic calcite and the diagenetic overgrowth.

3.3. The $\delta^{18}O$ and Mg/Ca Ratios of Crystallite Infillings

[17] A crystallite (~100 µm) was found infilling a chamber in the shell of the PETM morphotype *Morozovella allisonensis* (Figure 5a). The $\delta^{18}O$ composition of the infilling was measured twice with SIMS (~3–4 µm) beam spots (Figure 5b). These two in situ analyses yielded an average $\delta^{18}O$ value (1.4‰) that falls squarely within the range of $\delta^{18}O$ values reported above for the larger crystallites

cementing foraminiferal shells (Figure 2b). Two parallel traverses of Mg/Ca ratios analyzed by EPMA crosscutting the infilling crystallite show highest ratios in the core and a pattern of symmetrically decreasing values toward the rim (Figure 5c). The range of Mg/Ca ratios (~1 to ~10 mmol/mol) measured in the infilling crystallite is similar to that measured in the larger crystallites (see Figure 4c).

3.4. Intrashell Geochemical Variation in Uncemented Planktic Foraminifera

[18] The increased spatial resolution afforded by the smaller (~3 μm) SIMS beam spot permitted mapping of $\delta^{18}O$ variation along a transect running from the chamber wall across the muricae basal mound and up through the major axis of the muricae blades within a loose, uncemented planktic foraminiferal (*Morozovella velascoensis*) shell (Figures 5d–5f) exhibiting a state of preservation similar to that of specimens routinely selected for SST reconstructions [*Bralower et al*., 1995; *Tripati et al*., 2003]. A considerable degree of variation occurs along this transect with the basal mound of the muricae yielding the lowest $\delta^{18}O$ values centered on −3.3‰ (Figure 5g). By comparison, the $\delta^{18}O$ of the inner chamber wall is ~1‰ higher than that of the muricae basal mound. The highest $\delta^{18}O$ values of -1.2 to -0.1‰ were measured in the muricae blade (Figure 5g), which are 3‰ higher than the muricae base and only slightly lower than those registered by the diagenetic crystallites (0.1 to 2.9‰). Thus, the transition from the basal mound of the muricae into the muricae blade is marked by a precipitous increase of ~3.1‰ over a spatial distance of only ~5 μm along the SIMS-generated $\delta^{18}O$ traverse (Figures 5f and 5g).

[19] Complementary Mg/Ca ratios were measured in situ by EPMA along a traverse paralleling the SIMS $\delta^{18}O$ traverse running from the chamber wall across the muricae basal mound and up through the major axis of the muricae blade (Figure 5f). The Mg/Ca ratios vary between 2.3 and 4.7 mmol/mol within the chamber wall and basal portion of the muricae, averaging 3.1 mmol/mol, but abruptly increase to a peak value of 12.5 mmol/mol across the boundary between the basal mound and blade of the muricae (Figure 5g). This abrupt increase in Mg content occurs over the same boundary delimited by the sharp ~3.1‰ increase in $\delta^{18}O$. The increase in Mg/Ca ratios across this boundary is not as sharply defined as in the $\delta^{18}O$ transect as intermediate Mg/Ca ratios are recorded. This difference between the $\delta^{18}O$ and Mg/Ca profiles likely reflects an analytical "averaging effect" caused by overlapping EPMA measurements along undulating surfaces and/or fluorescence outside the beam spot. The range of Mg/Ca ratios (~2 to 12.5 mmol/mol) measured along the EPMA traverse spanning the chamber wall and muricae blade of the *M. velascoensis* shell is comparable to that measured in both the diagenetic infilling and larger crystallites.

4. Discussion

4.1. Carbonate Diagenesis Within Deep-Sea Sediments During the PETM

[20] The average $\delta^{18}O$ value of the six large crystallites (1.2‰ PDB) is consistent with $\delta^{18}O$ values predicted by numerical models for diagenetic calcite formed at cold, bottom water temperatures [*Schrag et al*., 1995; *Schrag*, 1999; *Tripati et al*., 2003]. By comparison, the $\delta^{18}O$ measured in the basal mounds of the muricae in planktic foraminiferal shells cemented to the crystallites (−3.6‰ PDB) is comparable to the $\delta^{18}O$ of age-equivalent unaltered "glassy" planktic foraminiferal shells preserved in clay-rich coastal plain deposits [*Pearson et al*., 2007] and is therefore considered to represent biogenic calcite that formed at sea surface temperatures of ~30°C [*Pearson et al*., 2001; *Kozdon et al*., 2011]. Thus, the bimodal distribution of SIMS $\delta^{18}O$ data compiled from the crystallites and the foraminiferal shell fragments cemented to them signals the presence of two very different phases of carbonate, a high $\delta^{18}O$ diagenetic end-member and a low $\delta^{18}O$ biogenic end-member (Figure 2b).

[21] The presence of crystallites within the Site 865 section provides a unique opportunity for assessing the timing and geochemical conditions under which postdepositional diagenesis occurred. Their large size and well-developed crystal faces suggest growth prior to substantial degrees of burial compaction. Moreover, the focused stratigraphic distribution of the crystallites clearly signals an association with PETM conditions, which seems plausible given that the carbonate saturation state of the ocean varied dramatically in response to massive carbon input and sequestration during this transient climate state [*Dickens et al*., 1997; *Zachos et al*., 2005; *Kelly et al*., 2010].

[22] The $\delta^{18}O$ of the crystallites averages 1.2‰ (PDB) and is higher than previously modeled values of ≤0.9‰ for diagenetic calcite that formed during the early Paleogene in tropical pelagic deep-sea sediments [*Schrag et al*., 1995; *Schrag*, 1999; *Tripati et al*., 2003]. Previous studies report peak PETM temperatures for intermediate waters of ~18–20°C [*Tripati and Elderfield*, 2005] at Site 865, followed by a subsequent cooling of 5–6°C [*Zachos et al*., 2001]. Assuming that the crystallites formed during the PETM recovery period at temperatures ≤12°C, then an average $\delta^{18}O$ of 1.2‰ (PDB) of the crystallites requires ambient waters with a $\delta^{18}O$ of at least 0.5‰ (SMOW). Such a high $\delta^{18}O$ value for intermediate waters surrounding the guyot may seem unrealistic since mean ocean $\delta^{18}O_{seawater}$ during an essentially ice-free world was close to −1.2‰ (SMOW) [*Zachos et al*., 2001]. Nonetheless, elevated intermediate water $\delta^{18}O$ values (~0.5‰) have been modeled for the PETM using paired Mg/Ca and $\delta^{18}O$ ratios of benthic and planktic foraminiferal shells from Site 865 [*Tripati and Elderfield*, 2005]. Moreover, downhole measurements of pore water $\delta^{18}O$ through the upper ~105 m of the hole 865B section yield values (~0.2‰ to ~0.8‰ SMOW) that are substantially higher than the $\delta^{18}O$ of modern intermediate water (−0.17‰) in this region [*Paull et al*., 1995]. Thus, comparable conditions with elevated pore water $\delta^{18}O$ may have prevailed during the PETM.

[23] Unlike the $\delta^{18}O$ offset measured between diagenetic and biogenic calcites, the distribution of Mg/Ca ratios compiled from the diagenetic crystallites is indistinguishable from that of the attached foraminiferal shell fragments (Figure 4c). Moreover, the average Mg/Ca ratio (6.2 mmol/mol) herein reported for the diagenetic crystallites is more than an order of magnitude lower than that predicted by inorganic precipitation experiments [*Mucci*, 1987; *Oomori et al*., 1987; *Erez*, 2003]. Similar low Mg contents approaching biogenic values have also been reported in recrystallized carbonates associated with a dissolution horizon in a deep-sea

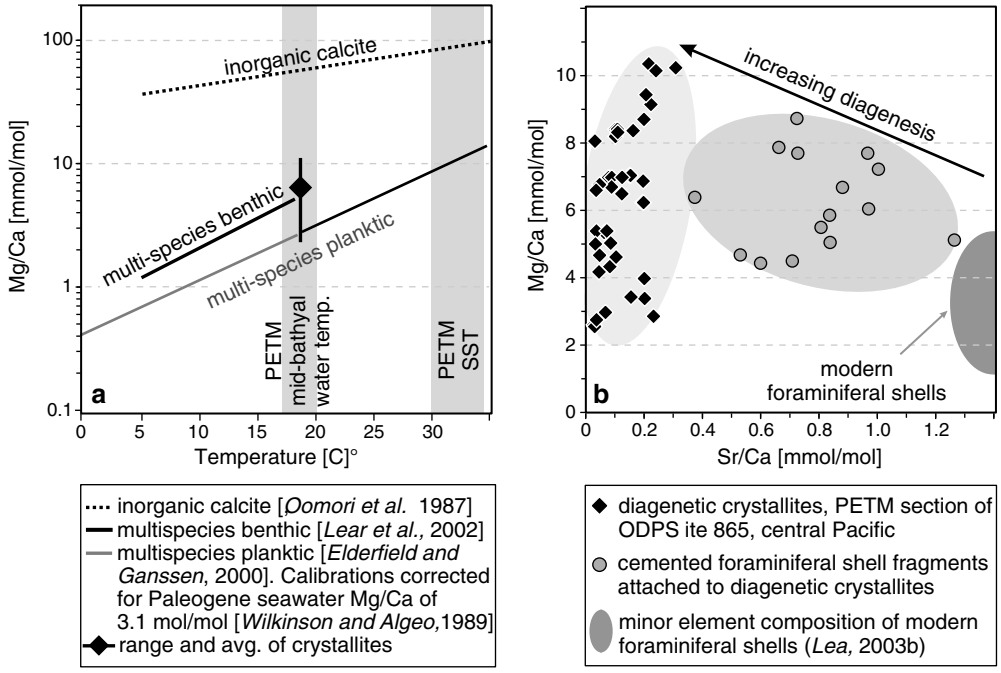

Figure 6. (a) Comparison of Mg/Ca ratios measured in the diagenetic crystallites to the Mg/Ca-temperature calibration curves for multiple species of modern planktic and benthic foraminifera and inorganic calcite precipitates grown in the laboratory. Dashed line is extrapolation beyond the calibrated temperature range. The Mg/Ca-temperature calibration curves for benthic and planktic foraminifera were adjusted for the lower Mg content of Paleogene seawater (Mg/Ca = 3.1 mol/mol, *Wilkinson and Algeo*, 1989) using the power law described by *Evans and Müller* [2012]. The grey vertical bars connote estimated PETM temperatures at Site 865 for intermediate [*Tripati and Elderfield*, 2005] and surface waters [*Pearson et al*., 2001; *Kozdon et al*., 2011]. (b) Bivariate plot comparing the Mg/Ca and Sr/Ca ratios of diagenetic crystallites and cemented foraminiferal shell fragments to the range of Mg/Ca and Sr/Ca ratios reported in modern planktic foraminiferal shells [*Lea*, 2003b].

section (Deep Sea Drilling Project Site 305) recovered from the northern Pacific Ocean [*Matter et al*., 1975; *Baker et al*., 1982].

[24] The relatively low Mg/Ca ratios of diagenetic calcite may, in part, be due to the presence of organic compounds, which can alter the partitioning coefficient of the minor elements [*Morse and Bender*, 1990]. However, another viable process for explaining the relatively low Mg contents of diagenetic calcite involves postdepositional dissolution of sedimentary calcite. The role of postdepositional dissolution in determining the Mg/Ca ratios of diagenetic calcite is not well constrained; still it is clear that the dissolution of biogenic calcite within the sediment column is the primary source of carbonate in the formation of diagenetic reprecipitates [e.g., *Wise*, 1977]. Here we note that the PETM interval containing the diagenetic crystallites is coincident with a pervasive dissolution horizon in deep-sea sedimentary records, which reflects shoaling of the lysocline in response to carbon input [*Dickens et al*., 1997; *Zachos et al*., 2005]. An important corollary is that lysocline shoaling promoted chemical erosion of sedimentary calcite exposed along the seafloor at locations such as Site 865 during the PETM. This dissolution front penetrated beneath the seafloor into the upper reaches of the sediment column, a phenomenon referred to as burndown [*Walker and Kasting*, 1992; *Dickens*, 2000]. Burndown into the sediment column continues until carbonate saturation is achieved within the interstitial pore waters, at which point the dissolved carbonate reprecipitates to form diagenetic cements and crystallites.

[25] We therefore view the crystallites as being diagenetic reprecipitates with an amalgamated chemical composition inherited from less stable, "donor" phases of carbonate that underwent solution in the sediment column. This form of geochemical inheritance is supported by comparison of the Mg/Ca ratios measured in the diagenetic crystallites to the Mg/Ca-temperature calibration curves for multiple species of modern planktic and benthic foraminifera and experimental inorganic calcite precipitates grown in the laboratory (Figure 6a). The Mg/Ca ratios of the diagenetic crystallites closely match those predicted for foraminiferal shells calcified during the late Paleocene and PETM. This congruence is consistent with the view that the crystallites are reprecipitates from carbonate dissolved during the precursory "burndown" event and partially reflect the original Mg content of previously deposited foraminiferal shells that underwent solution in the sediment column. This being the case, then it stands to reason that geochemical inheritance may help explain why the addition of diagenetic calcite to foraminiferal shells during postdepositional alteration does not significantly change the original biogenic Mg/Ca ratio.

[26] Our results indicate that Mg/Ca ratios are not a reliable indicator of diagenesis, but there are a few notable exceptions. For instance, Mg/Ca ratios measured in diagenetic infillings of foraminiferal shells recovered from the eastern

Mediterranean Sea approach the tenfold higher Mg/Ca ratio predicted by inorganic precipitation experiments [*Boussetta et al*., 2011]. The relatively elevated Mg/Ca ratios reported for these infillings may reflect the atypical seawater chemistry in this particular region [*Milliman and Müller*, 1973]; nevertheless, this exception indicates that the effects of diagenetic alteration on the geochemical composition of biogenic calcite should be evaluated on a site-specific basis [*Delaney*, 1989].

[27] The Sr/Ca ratios show a distinct trend toward lower values with increasing levels of diagenesis (Figure 6b). This is most evident when the Sr/Ca ratios for the diagenetic crystallites and cemented (moderately altered) foraminiferal shell fragments are compared to those of modern, unaltered planktic foraminiferal shells (Figure 6b). Sr/Ca ratios decrease progressively with increasing degrees of alteration as delineated by the decline from high, uniform values of modern, unaltered shells (~1.2 to 1.6 mmol/mol [*Lea*, 2003a]) to intermediate, variable values for cemented foraminiferal shell fragments to the lowest values (≤0.3 mmol/mol) for the diagenetic crystallites. Thus, the Sr/Ca ratios herein reported support earlier studies suggesting the use of Sr/Ca ratios to assess foraminiferal preservation because Sr/Ca ratios of biogenic foraminiferal calcite are relatively high and uniform, while the ratios of diagenetic calcite are typically lower and more variable [*Baker et al*., 1982; *Ando et al*., 2010].

4.2. Intrashell $\delta^{18}O$ and Mg/Ca Compositional Trends

[28] The striking 4.8‰ offset between the $\delta^{18}O$ values of the crystallites and cemented foraminiferal shell fragments indicates that even moderate diagenetic alteration can have a significant impact on whole-shell $\delta^{18}O$ of planktic foraminifera (Figure 2b). As previously discussed, this raises several questions regarding the fidelity of published SST records derived from "whole-shell" acid-digestion analytical techniques using frosty planktic foraminifera. An earlier study revealed that the basal, mound-like areas of muricae are less porous than the remaining shell and have a generally higher resistance to diagenetic alteration [*Kozdon et al*., 2011]. This finding also led to the supposition that the calcite blades emanating from the muricae mounds may represent diagenetic overgrowths with a higher $\delta^{18}O$ than the remaining shell (Figures 5d–5f), biasing paleoceanographic records toward erroneously colder SSTs when the whole shell is analyzed by conventional methods [*Sexton et al*., 2006; *Kozdon et al*., 2011].

[29] These interpretations are validated by the coherent trends seen in the $\delta^{18}O$ and Mg/Ca traverses running from the chamber wall up through the major axis of a muricae blade in a planktic foraminiferal (*Morozovella velascoensis*) shell (Figures 5d–5f). The low $\delta^{18}O$ values centered on −3.3‰ acquired from the basal mound of the muricae are comparable to those reported for age-equivalent glassy shells from other locations [*Pearson et al*., 2007], indicating that this domain is relatively resistant to alteration and an optimal target for extracting paleoceanographic information (Figure 5g) [*Kozdon et al*., 2011]. The slightly higher $\delta^{18}O$ values registered for the chamber wall suggest a moderate degree of alteration most likely facilitated by the higher porosity and microgranular structure of this domain, while the diagenetic origin of the muricae blade is confirmed by its higher $\delta^{18}O$ values (Figures 5f and 5g). A diagenetic origin for the muricae blade is also supported by the elevated Mg content of this domain relative to the low Mg biogenic calcite formed by planktic foraminifera (Figures 5f and 5g). This view is further substantiated by the fact that the crystallites and muricae blade yield similar peak Mg/Ca ratios (~10 to 12.5 mmol/mol), although the Mg content increases associated with these diagenetic phases are still more than threefold lower than those predicted by experimental studies [*Katz*, 1973; *Mucci*, 1987; *Oomori et al*., 1987; *Erez*, 2003]. Thus, the transition from biogenic calcite in the basal mound of the muricae to diagenetic calcite in the muricae blade is delimited by sharp increases in both $\delta^{18}O$ and Mg/Ca ratios over a spatial distance of only ~5 μm (Figures 5f and 5g). The intrashell compositional trends delineated in this study also provide sorely needed insight into why the Mg/Ca ratios in frosty planktic foraminiferal shells are only slightly elevated compared to those of their glassy counterparts [*Sexton et al*., 2006; *Kozdon et al*., 2011].

[30] The $\delta^{18}O$ and Mg/Ca traverses spanning the chamber wall and muricae indicate that the pustular biogenic mounds on the surface of morozovellid and acarininid shells serve as nucleation sites for cementation [*Sexton et al*., 2006] that result in the postdepositional formation of enlarged blades. Why this is the case remains unclear, although it has been speculated that aspects such as crystallographic orientation, availability of specific crystal planes for secondary overgrowth, and/or residual organic matter may play a role in the preferential alteration of specific domains within foraminiferal shells [*Boussetta et al*., 2011]. Comparison of the in situ $\delta^{18}O$ data acquired from the crystallites to that obtained from the muricae blade may provide some insight into this diagenetic process. Specifically, we note that the $\delta^{18}O$ values of the muricae blade (−1.2 to −0.1‰) are lower than those measured from the crystallites (0.1 to 2.9‰). This difference may indicate that minor amounts of ^{18}O-depleted, biogenic calcite in the form of delicate "spine-like" protuberances are subsumed within the enlarged muricae blades and/or that the muricae blades formed at a different time under dissimilar conditions than the crystallites.

[31] The latter of these two explanations is supported by the fact that unlike the short stratigraphic interval over which the large crystallites occur, muricae blades are commonplace on planktic foraminiferal shells throughout the entire early Paleogene sedimentary record and are prominent "morphological features" on shells belonging to the mixed-layer dwelling genera *Acarinina* and *Morozovella* [*Blow*, 1979; *Berggren and Norris*, 1997; *Olsson et al*., 1999; *Pearson et al*., 2006]. It was not until the discovery of well-preserved "glassy" Paleogene planktic foraminifera from Tanzanian drill cores [*Pearson et al*., 2001] that a diagenetic origin for these blade-shaped muricae tips was postulated [*Sexton et al*., 2006]. We also note that previous studies [*Kelly et al*., 1996, 1998] have shown that the stratigraphy of the Site 865 PETM record has been strongly influenced by sediment mixing, raising the possibility that the shell from which the muricae blade $\delta^{18}O$ and Mg/Ca data were acquired may have been reworked from slightly older sediments up into the PETM interval. Thus, the muricae blades on the *M. velascoensis* shell targeted for SIMS and EPMA analyses may have formed at a different time and/or under different conditions than the large crystallites.

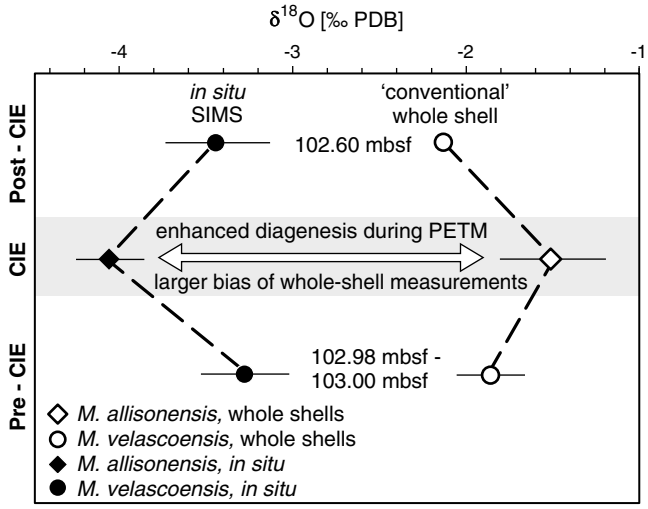

Figure 7. Comparison of published planktic foraminiferal oxygen isotope ratios encompassing the CIE in the Site 865C PETM section. Data from conventional phosphoric-acid whole-shell measurements are from *Kelly et al*. [1996] and *Bralower et al*. [1995], and in situ SIMS analyses of alteration-resistant domains within planktic foraminiferal shells are from *Kozdon et al*. [2011]. Error bars show 1 standard deviation of multiple measurements from the same core sample.

4.3. Implications for Tropical Sea Surface Temperature Records

[32] The deleterious effects of postdepositional diagenesis on SST records are manifested in the literature as the "cool tropics paradox" whereby planktic foraminiferal $\delta^{18}O$ records for the Cretaceous and Paleogene greenhouse climate states signal little, to no, warming in the tropics while correlative high-latitude SST records register marked increases [*D'Hondt and Arthur*, 1996; *Pearson et al*., 2001]. The $\delta^{18}O$ records upon which the cool tropics paradox is based were generated using conventional techniques that necessitate acid digestion of whole shells with the assumption that the chemistries of fossil foraminifera are homogeneous and well preserved, yet the in situ $\delta^{18}O$ and Mg/Ca data clearly show that the frosty planktic foraminiferal shells are aggregate mixtures of primary biogenic and secondary diagenetic calcite (Figures 5d–5g). Moreover, we have found that diagenesis can occur as infillings within the chambers of foraminiferal shells that are easily overlooked when specimens for paleoceanographic studies are selected by binocular microscopy [e.g., *Barrera et al*., 1987; *Schrag et al*., 1992]. Application of in situ techniques clearly shows that the $\delta^{18}O$ and Mg/Ca ratios of such diagenetic infilling differ from those of the biogenic calcite (Figures 5a–5c) and are highly congruous with the $\delta^{18}O$ and Mg/Ca ratios measured in the larger crystallites cementing foraminiferal shells (Figures 2a, 2b, 3a–3c, and 4a–4c). This congruence suggests the concurrent formation of the diagenetic infilling and larger crystallites after the "burndown" event associated with the PETM. Collectively, these lines of evidence corroborate the view that the cool tropics paradox is largely an aberration stemming from the diagenetic overprinting of foraminiferal shells [*Pearson et al*., 2001; *Sexton et al*., 2006; *Pearson et al*., 2007].

[33] The results of this study also indicate that the degree of diagenetic alteration to planktic foraminiferal shells is not uniform throughout the sediment column, which can further complicate paleoclimate records derived from the $\delta^{18}O$ of whole-shell measurements. For example, whole-shell $\delta^{18}O$ values of the PETM morphotype *Morozovella allisonensis* are generally higher than those of contemporaneous *M. velascoensis* shells at Site 865 [*Kelly et al*., 1996]. This interspecies $\delta^{18}O$ offset was originally attributed to differences in the preferred depth ecologies of the two species, with *M. allisonensis* occupying a deeper depth habitat than *M. velascoensis* [*Kelly et al*., 1996]. However, in situ $\delta^{18}O$ measurements of alteration-resistant domains within shells of these two species yield contradictory results with the lowest $\delta^{18}O$ values being registered by the PETM morphotype *M. allisonensis* (Figure 7). This finding suggests that diagenetic overprinting of planktic foraminiferal shells may have been more severe during the transient PETM, an interpretation wholly consonant with the postdepositional dissolution-reprecipitation model herein described.

5. Conclusions

[34] The unparalleled spatial resolution afforded by in situ SIMS and EPMA techniques, in combination with careful sample preparation and imaging, can be successfully applied to delineate $\delta^{18}O$ and elemental ratio (Mg/Ca, Sr/Ca) compositional trends within diagenetic crystallites and individual frosty planktic foraminiferal shells preserved in deep-sea sediments. In detail, we use these analytical approaches to (1) identify domains within frosty planktic foraminifera that retain the original shell chemistry, (2) measure the $\delta^{18}O$ and minor element (Mg/Ca, Sr/Ca) compositions of both the diagenetic end-member calcite and the unaltered to moderately altered biogenic calcite in frosty planktic foraminiferal shells, and (3) verify that the "cool tropics paradox" is largely an artifact of bulk analysis and diagenesis. An important corollary to these findings is that the dissolution of sedimentary calcite (burndown) followed by the reprecipitation of ^{18}O-rich carbonate on planktic foraminiferal shells within the sediment column can effectively mask the $\delta^{18}O$ decrease signaling warmer tropical SSTs during the PETM. Thus, in situ analytical techniques hold much promise for enhancing the quality of ocean-climate records derived from the shell chemistries of frosty planktic foraminifera that pervade the deep-sea sedimentary archive.

[35] **Acknowledgments.** This research was supported by NSF OCE-1131516, the Wisconsin Alumni Research Foundation to D.C.K., and the U.W. Weeks Fund. Brian Hess prepared the sample mounts. Reviews by Philip Sexton and two anonymous reviewers substantially improved this paper. We thank Heiko Pälike for editorial handling. WiscSIMS is partially supported by NSF-EAR-1053466.

References

Ando, A., B. T. Huber, and K. G. MacLeod (2010), Depth-habitat reorganization of planktonic foraminifera across the Albian/Cenomanian boundary, *Paleobiology*, *36*(3), 357–373, doi:10.1666/09027.1.

Baker, P. A., J. M. Gieskes, and H. Elderfield (1982), Diagenesis of carbonates in deep-sea sediments—Evidence from Sr/Ca ratios and interstitial dissolved Sr^{2+} data, *J. Sediment. Petrol.*, *52*, 71–82.

Barrera, E., B. T. Huber, S. M. Savin, and P.-N. Webb (1987), Antarctic marine temperatures: Late Campanian through early Paleocene, *Paleoceanography*, *2*(1), 21–47, doi:10.1029/PA002i001p00021.

Berggren, W. A., and R. D. Norris (1997), Biostratigraphy phylogeny and systematics of Paleocene trochospiral planktic foraminifera, *Micropaleontology*, *43*, 1–116.

Blow, W. H. (1979), *The Cainozoic Globigerinida*, E. J. Brill, Leiden.

Boussetta, S., F. Bassinot, A. Sabbatini, N. Caillon, J. Nouet, N. Kallel, H. Rebaubier, G. Klinkhammer, and L. Labeyrie (2011), Diagenetic Mg-rich calcite in Mediterranean sediments: Quantification and impact on foraminiferal Mg/Ca thermometry, *Mar. Geol.*, *280*(1–4), 195–204, doi:10.1016/j.margeo.2010.12.011.

Bralower, T. J., and J. Mutterlose, (1995), Calcareous nannofossil biostratigraphy of Site 865, Allison Guyot, Central Pacific Ocean: A tropical Paleogene reference section, in *Proceedings of the Ocean Drilling Program, Scientific Results*, edited by E. L. Winterer et al., pp. 31–74, Ocean Drilling Program, College Station, TX.

Bralower, T. J., J. C. Zachos, E. Thomas, M. Parrow, C. K. Paull, D. C. Kelly, I. P. Silva, W. V. Sliter, and K. C. Lohmann (1995), Late Paleocene to Eocene paleoceanography of the equatorial Pacific Ocean: Stable isotopes recorded at Ocean Drilling Program Site 865, Allison Guyot, *Paleoceanography*, *10*(4), 841–865.

Cavosie, A. J., J. W. Valley, S. A. Wilde, and E.I.M.F (2005), Magmatic $\delta^{18}O$ in 4400–3900 Ma detrital zircons: A record of the alteration and recycling of crust in the Early Archean, *Earth Planet. Sci. Lett.*, *235*(3–4), 663–681, doi:10.1016/j.epsl.2005.04.028.

Coplen, T. B., C. Kendall, and J. Hopple (1983), Comparison of stable isotope reference samples, *Nature*, *302*, 236–238.

Delaney, M. L. (1989), Temporal changes in interstitial water chemistry and calcite recrystallization in marine sediments, *Earth Planet. Sci. Lett.*, *95*, 23–37.

D'Hondt, S., and M. A. Arthur (1996), Late Cretaceous oceans and the cool tropic paradox, *Science*, *271*, 1838–1841.

Dickens, G. R. (2000), Methane oxidation during the late Palaeocene thermal maximum, *Bull. Soc. Geol. Fr.*, *171*(1), 37–49.

Dickens, G. R., M. M. Castillo, and J. C. G. Walker (1997), A blast of gas in the latest Paleocene: Simulating first-order effects of massive dissociation of oceanic methane hydrate, *Geology*, *25*(3), 259–262, doi:10.1130/0091-7613(1997)025<0259:abogit>2.3.co;2.

Elderfield, H., and G. Ganssen (2000), Past temperature and $\delta^{18}O$ of surface ocean waters inferred from foraminiferal Mg/Ca ratios, *Nature*, *405*, 442–445.

Erez, J. (2003), The source of ions for biomineralization in foraminifera and their implications for paleoceanographic proxies, *Rev. Mineral. Geochem.*, *54*, 115–149.

Evans, D., and W. Müller (2012), Deep time foraminifera Mg/Ca paleothermometry: Nonlinear correction for secular change in seawater Mg/Ca, *Paleoceanography*, *27*, PA4205, doi:10.1029/2012PA002315.

Katz, A. (1973), The interaction of magnesium with calcite during crystal growth at 25–90°C and one atmosphere, *Geochim. Cosmochim. Acta*, *37*, 1563–1586.

Kelly, D. C., T. J. Bralower, J. C. Zachos, I. P. Silva, and E. Thomas (1996), Rapid diversification of planktonic foraminifera in the tropical Pacific (ODP Site 865) during the late Paleocene thermal maximum, *Geology*, *24*(5), 423–426.

Kelly, D. C., T. J. Bralower, and J. C. Zachos (1998), Evolutionary consequences of the latest Paleocene thermal maximum for tropical planktonic foraminifera, *Palaeogeogr. Palaeoclimatol. Palaeoecol.*, *141*, 139–161.

Kelly, D. C., T. M. J. Nielsen, H. K. McCarren, J. C. Zachos, and U. Röhl (2010), Spatiotemporal patterns of carbonate sedimentation in the South Atlantic: Implications for carbon cycling during the Paleocene–Eocene thermal maximum, *Palaeogeogr. Palaeoclimatol. Palaeoecol.*, *293*(1–2), 30–40, doi:10.1016/j.palaeo.2010.04.027.

Killingley, J. S. (1983), Effects of diagenetic recrystallization on $^{18}O/^{16}O$ values of deep-sea sediments, *Nature*, *301*, 594–597.

Kita, N. T., T. Ushikubo, B. Fu, and J. W. Valley (2009), High precision SIMS oxygen isotope analysis and the effect of sample topography, *Chem. Geol.*, *264*(1–4), 43–57, doi:10.1016/j.chemgeo.2009.02.012.

Kozdon, R., T. Ushikubo, N. T. Kita, M. Spicuzza, and J. W. Valley (2009), Intratest oxygen isotope variability in the planktonic foraminifer *N. pachyderma*: Real vs. apparent vital effects by ion microprobe, *Chem. Geol.*, *258*, 327–337, doi:10.1016/j.chemgeo.2008.10.032.

Kozdon, R., D. C. Kelly, N. T. Kita, J. H. Fournelle, and J. W. Valley (2011), Planktonic foraminiferal oxygen isotope analysis by ion microprobe technique suggests warm tropical sea surface temperatures during the Early Paleogene, *Paleoceanography*, *26*, PA3206, doi:10.1029/2010PA002056.

Lea, D. W. (2003a), Elemental and isotopic proxies of past ocean temperatures, in *Treatise on Geochemistry: The Oceans and Marine Geochemistry*, edited by H. Elderfield, pp. 365–390, Elsevier, New York.

Lea, D. W. (2003b), Trace elements in foraminiferal calcite, in *Modern Foraminifera*, edited by B. Sen Gupta, pp. 259–277, Springer, Netherlands.

Matter, A., R. G. Douglas, and K. Perch-Nielsen (1975), Fossil preservation, geochemistry, and diagenesis of pelagic carbonates from Shatsky Rise, Northwest Pacific, in *Initial Reports of the Deep Sea Drilling Project*, edited by R. L. Larson and R. Moberly, pp. 891–921, U.S. Government Printing Office, Washington D.C.

Matthews, R. K., and R. Z. Poore (1980), Tertiary δ18O record and glacio-eustatic sea-level fluctuations, *Geology*, *8*(10), 501–504, doi:10.1130/0091-7613(1980)8<501:torags>2.0.co;2.

Milliman, J. D., and J. Müller (1973), Precipitation and lithification of magnesian calcite in the deep-sea sediments of the eastern Mediterranean Sea, *Sedimentology*, *20*(1), 29–45, doi:10.1111/j.1365-3091.1973.tb01605.x.

Morse, J. W., and M. L. Bender (1990), Partition coefficients in calcite: Examination of factors influencing the validity of experimental results and their application to natural systems, *Chem. Geol.*, *82*, 265–277, doi:10.1016/0009-2541(90)90085-l.

Mucci, A. (1987), Influence of temperature on the composition of magnesian calcite overgrowth precipitated from seawater, *Geochim. Cosmochim. Acta*, *51*, 1977–1984.

Norris, R. D., and P. A. Wilson (1998), Low-latitude sea-surface temperatures for the mid-Cretaceous and the evolution of planktic foraminifera, *Geology*, *26*(9), 823–826.

Olsson, R. K., W. A. Berggren, C. Hemleben, and B. T. Huber (1999), *Atlas of Paleocene Planktonic Foraminifera*, 252 pp., Smithsonian Institution Press, Washington, D.C.

Oomori, T., H. Kaneshima, Y. Maezato, and Y. Kitano (1987), Distribution coefficient of Mg^{2+} ions between calcite and solution at 10–50°C, *Mar. Chem.*, *20*, 327–336.

Paull, C. K., P. D. Fullagar, T. J. Bralower, and U. Röhl (1995), Seawater ventilation of Mid-Pacific guyots drilled during Leg 143, in *Proceedings of the Ocean Drilling Program, Scientific Results*, edited by E. L. Winterer et al., pp. 231–241, Ocean Drilling Program, College Station, TX.

Pearson, P. N. (2012), Oxygen isotopes in foraminifera: Overview and historical review, in *Reconstructing the Earth's Deep-Time Climate—The State of the Art in 2012*, edited by L. C. Ivany and B. T. Huber, pp. 1–38, The Paleontological Society, Cardiff, U.K.

Pearson, P. N., and C. E. Burgess (2008), Foraminifer test preservation and diagenesis: Comparison of high latitude Eocene sites, in *Biogeochemical Controls on Palaeoceanographic Environmental Proxies*, edited by W. E. N. Austin and R. H. James, pp. 59–72, Geological Society, London, Special Publications.

Pearson, P. N., P. W. Ditchfield, J. Singano, K. G. Harcourt-Brown, C. J. Nicholas, R. K. Olsson, N. J. Shackleton, and M. Hall (2001), Warm tropical sea surface temperatures in the Late Cretaceous and Eocene epochs, *Nature*, *413*, 481–487.

Pearson, P. N., R. K. Olsson, C. Hemleben, B. T. Huber, and W. A. Berggren (2006), *Atlas of Eocene Planktonic Foraminifera*, pp. 513, Cushman Foundation Special Publication, Lawrence, Kansas.

Pearson, P. N., B. E. van Dongen, C. J. Nicholas, R. D. Pancost, S. Schouten, J. M. Singano, and B. S. Wade (2007), Stable warm tropical climate through the Eocene epoch, *Geology*, *35*(3), 211–214.

Sager, W. W., E. L. Winterer, and J. V. Firth (1993), Proceedings of the Ocean Drilling Program. Initial Report 143.

Schrag, D. P. (1999), Effects of diagenesis on the isotopic record of late Paleogene tropical sea surface temperatures, *Chem. Geol.*, *161*(1–3), 215–224, doi:10.1016/s0009-2541(99)00088-1.

Schrag, D. P., D. J. DePaolo, and F. M. Richter (1992), Oxygen isotope exchange in a two-layer model of oceanic crust, *Earth Planet. Sci. Lett.*, *111*, 305–317.

Schrag, D. P., D. J. DePaolo, and F. M. Richter (1995), Reconstructing past sea surface temperatures: Correcting for diagenesis of bulk marine carbonate, *Geochim. Cosmochim. Acta*, *59*, 2265–2278.

Sexton, P. F., P. A. Wilson, and P. N. Pearson (2006), Microstructural and geochemical perspectives on planktic foraminiferal preservation: "Glassy" versus "frosty", *Geochem. Geophys. Geosyst.*, *7*, Q12P19, doi:10.1029/2006GC001291.

Tripati, A., and H. Elderfield (2005), Deep-sea temperature and circulation changes at the Paleocene-Eocene thermal maximum, *Science*, *308*, 1894–1898.

Tripati, A. K., M. L. Delaney, J. C. Zachos, L. D. Anderson, D. C. Kelly, and H. Elderfield (2003), Tropical sea-surface temperature reconstruction for the early Paleogene using Mg/Ca ratios of planktonic foraminifera, *Paleoceanography*, *18*(4), 1101, doi:10.1029/2003PA000937.

Valley, J. W., and N. T. Kita (2009), In situ oxygen isotope geochemistry by ion microprobe, in *MAC Short Course: Secondary Ion Mass Spectrometry in the Earth Sciences*, edited by M. Fayek, pp. 16–63, Mineralogical Association of Canada Short Course 41, Toronto.

Vetter, L., R. Kozdon, C. I. Mora, S. M. Eggins, J. W. Valley, B. Hönisch, and H. J. Spero (2013), Micron-scale intrashell oxygen isotope variation

in cultured planktic foraminifers, *Geochim. Cosmochim. Acta*, *107*(0), 267–278, doi:10.1016/j.gca.2012.12.046.

Walker, J. C. G., and J. F. Kasting (1992), Effects of fuel and forest conservation on future levels of atmospheric carbon dioxide, *Palaeogeogr. Palaeoclimatol. Palaeoecol.*, *97*(3), 151–189, doi:10.1016/0031-0182(92)90207-l.

Wilkinson, B. H., and T. J. Algeo (1989), Sedimentary carbonate record of Ca-Mg cycling at the Earth's surface, *Am. J. Sci.*, *289*, 1158–1194.

Wilson, P. A., and R. D. Norris (2001), Warm tropical ocean surface and global anoxia during the mid-Cretaceous period, *Nature*, *412*(6845), 425–429.

Wilson, P. A., R. D. Norris, and M. J. Cooper (2002), Testing the Cretaceous greenhouse hypothesis using glassy foraminiferal calcite from the core of the Turonian tropics on Demerara Rise, *Geology*, *30*(7), 607–610.

Wise, S. W. (1977), Chalk formation: Early diagenesis, in *The Fate of Fossil Fuel CO_2 in the Oceans*, edited by R. N. Anderson and A. Malahoff, pp. 717–739, Plenum Press, New York.

Zachos, J. C., M. Pagani, L. Sloan, E. Thomas, and K. Billups (2001), Trends, rhythms, and aberrations in global climate 65 Ma to present, *Science*, *292*, 686–693, doi:10.1126/science.1059412.

Zachos, J. C., et al. (2005), Rapid acidification of the ocean during the Paleocene-Eocene thermal maximum, *Science*, *308*(5728), 1611–1615, doi:10.1126/science.1109004.

Zachos, J. C., S. Schouten, S. Bohaty, T. Quattlebaum, A. Sluijs, H. Brinkhuis, S. J. Gibbs, and T. J. Bralower (2006), Extreme warming of mid-latitude coastal ocean during the Paleocene-Eocene thermal maximum: Inferences from TEX_{86} and isotope data, *Geology*, *34*(9), 737–740, doi:10.1130/G22522.1.